Biochemical and Biophysical Research Communications 436 (2013) 271–277

Contents lists available at SciVerse ScienceDirect

Biochemical and Biophysical Research Communications

journal homepage: www.elsevier.com/locate/ybbrc

# Deletion of the calmodulin-binding domain of Grb7 impairs cell attachment to the extracellular matrix and migration

Irene García-Palmero [1], Antonio Villalobo *

*Department of Cancer Biology, Instituto de Investigaciones Biomédicas, Consejo Superior de Investigaciones Científicas and Universidad Autónoma de Madrid, c/ Arturo Duperier 4, E-28029 Madrid, Spain*

ARTICLE INFO

*Article history:*
Received 22 May 2013
Available online 4 June 2013

*Keywords:*
Calmodulin
Cell migration
Cell adhesion
Cytoskeleton
Grb7

ABSTRACT

The adaptor Grb7 is a calmodulin (CaM)-binding protein that participates in signaling pathways involved in cell migration, proliferation and the control of angiogenesis, and plays a significant role in tumor growth, its metastatic spread and tumor-associated neo-vasculature formation. In this report we show that deletion of the CaM-binding site of Grb7, located in the proximal region of its pleckstrin homology (PH) domain, impairs cell migration, cell attachment to the extracellular matrix, and the reorganization of the actin cytoskeleton occurring during this process. Moreover, we show that the cell-permeable CaM antagonists *N*-(6-aminohexyl)-5-chloro-1-naphthalenesulfonamide (W-7) and *N*-(4-aminobutyl)-5-chloro-2-naphthalenesulfonamide (W-13) both retard the migration of cells expressing wild type Grb7, but not the migration of cells expressing the mutant protein lacking the CaM-binding site (Grb7Δ), underscoring the proactive role of CaM binding to Grb7 during this process.



## 1. Introduction

Grb7 is a mammalian adaptor protein that plays important roles in mediating the transmission of signals from tyrosine kinase receptors and cytoplasmic tyrosine kinases by coupling protein complexes. Grb7, Grb10 and Grb14 form a protein family [1–6] that is phylogenetically related to the *Caenorhabditis elegans* Mig10 protein, which is involved in the regulation of embryonic neural cell migration [7,8]. These proteins share significant sequence homology and a well conserved modular structure divided in several domains. Human Grb7 is a 532 amino acid protein harboring an amino-terminal proline-rich region; a central GM region (for Grb and Mig10) that includes three domains: RA, PH and BPS; and a C-terminal region formed by a SH2 domain [1–6].

Grb7 participates in integrin-mediated signaling pathways by interacting with FAK [9] and also binds to the EphB1 receptor [10], triggering in both cases cell migration. Upon FAK autophosphorylation at Tyr397, Grb7 interacts with the kinase through its SH2 domain resulting in its phosphorylation at Tyr188 and Tyr338 [11,12]. The interaction of the PH domain of Grb7 with phosphoinositides at the plasma membrane seems to be necessary for proper FAK-mediated Grb7 phosphorylation; however, the subsequent downstream signaling events are largely unknown [11].

Our laboratory described the presence of a CaM-BD in the proximal region of the PH domain of Grb7 [13], and demonstrated the relevance of this site in the translocation of Grb7 into the nucleus [14], and its role in tumor growth and tumor-associated angiogenesis *in vivo* [15]. We have shown that a Grb7 mutant lacking the CaM-BD (Grb7Δ) lost the ability to bind to membranes and different phosphoinositides, although partial binding to phosphatidyl-3-phosphate and phosphatidyl-3,5-bisphosphate remained [13]. In this report we show that deletion of the CaM-BD of Grb7 results in impaired cell migration, adhesion and reorganization of the actin cytoskeleton, suggesting that CaM is involved in these processes via a Grb7-mediated mechanism.

*Abbreviations:* AEBSF, 4-(2-aminoethyl)-benzenesulfonyl fluoride; CaM, calmodulin; CaM-BD, calmodulin-binding domain; BPS, between PH and SH2; DAPI, 4′,6-diamidino-2-phenylindole; DMEM, Dulbecco's modified Eagle's medium; E-64, *N*-[*N*-(L-3-trans-carboxyirane-2-carbonyl)-L-leucyl]-agmatine; ECL, enhanced chemiluminescence; EDTA, ethylene-diamine-tetraacetic acid; EGTA, ethylene-glycol-tetraacetic acid; EphB1, ephrin type-B receptor 1; ERK1/2, extracellular regulated kinases 1 and 2; FAK, focal adhesion kinase; FBS, fetal bovine serum; Grb7/10/14, growth factor receptor bound proteins 7, 10 and 14; NP-40, nonylphenoxypolyethoxylethanol; PH, pleckstrin homology; PBS, phosphate buffer saline; PMSF, phenylmethylsulfonyl fluoride; PVDF, poly(vinylidenedifluoride); RA, Ras-associating; SDS-PAGE, polyacrylamide gel electrophoresis in the presence of sodium dodecyl sulfate; SH2, Src homology 2; W-7, *N*-(6-aminohexyl)-5-chloro-1-naphthalenesulfonamide; W-13, *N*-(4-aminobutyl)-5-chloro-2-naphthalenesulfonamide.

* Corresponding author. Address: Instituto de Investigaciones Biomédicas CSIC-UAM, c/ Arturo Duperier 4, E-28029 Madrid, Spain. Fax: +34 91 585 4401.
*E-mail address:* antonio.villalobo@iib.uam.es (A. Villalobo).
[1] Present address: Centro de Investigaciones Biológicas, Consejo Superior de Investigaciones Científicas, c/ Ramiro de Maeztu 9, E-28040 Madrid, Spain.

0006-291X/$ - see front matter © 2013 Elsevier Inc. All rights reserved.
http://dx.doi.org/10.1016/j.bbrc.2013.05.092

## 2. Materials and methods

### 2.1. Reagents

Anti-Grb7 (N-20), anti-FAK and anti-phospho-FAK (Tyr397) rabbit polyclonal antibodies, and anti-phospho-ERK1/2 (Thr202/Tyr204) mouse monoclonal antibody were from Santa Cruz Biotechnology. Anti-ERK1/2 and anti-GAPDH rabbit monoclonal antibodies were from Cell Signaling Technology. Anti-rabbit IgG (goat) polyclonal antibody coupled to horseradish peroxidase was from Zymed Laboratories or Invitrogen. The anti-mouse Fc specific IgG polyclonal (goat) antibody coupled to horseradish peroxidase, EGTA and fibronectin (from bovine plasma) were from Sigma–Aldrich. PVDF membranes were from Pall Corporation, and DMEM, FBS, G418 (Geneticin), ProLong® Gold Antifade reagent, DAPI and Alexa Fluor® 488 phalloidin were from Invitrogen. The ECL kit was from GE Healthcare-Amersham, and the X-ray films from Konika Minolta. Glass-bottom culture dishes (35 mm diameter) coated with collagen or poly-D-lysine were from MatTek, the 6-wells Transwell® clusters equipped with 24 mm polycarbonate membranes (8 μm pore size) were from Corning Incorporated, andW-13 and W-7 were from Calbiochem.

### 2.2. Cell culture and transfection

Authenticated human embryonic kidney (HEK) 293 cells (ATCC® number CRL-1573™) were grown in DMEM supplemented with 10% (v/v) FBS, 2 mM L-glutamine, 40 μg/ml gentamicin (plus 1 mg/ml G418 for stable transfectants) at 37 °C in an humidified air atmosphere containing 5% $CO_2$. The cells (≈80% confluent) were treated with 25 μM chloroquine and transfected with pcDNA3.1 (empty vector), pcDNA3/FLAG-Grb7, pcDNA3/FLAG-Grb7Δ, pEYFP-Grb7 or pEYFP-Grb7Δin a medium containing 120 mM $CaCl_2$, 25 mM $Na_2HPO_4$, 150 mM KCl, 250 mM NaCl, 50 mM glucose and 25 mM Hepes-NaOH (pH 7.0). Stable transfectants were selected with 1 mg/ml G418 for 15–20 days and isolated using cloning rings and trypsin/EDTA. Grb7 and Grb7Δ expression was tested by Western blot using the anti-Grb7 (N-20) antibody. Control experiments were performed with cells transfected with the empty vector or non-transfected cells.

### 2.3. Preparation of cell extracts

Cells were washed twice with cold PBS and lysed with a buffer containing 50 mM Tris–HCl (pH 8), 150 mM NaCl, 1% (w/v) deoxycholic acid, 1% (v/v) NP-40, phosphatase inhibitors (100 mM NaF and 1 mM $Na_3VO_4$) and protease inhibitors (5 μM pepstatin A, 10 μM leupeptin, 0.5 mM AEBSF, 0.4 μM aprotinin, 7.5 μM E-64, 25 μM bestatin, and freshly prepared 1 mM PMSF). Lysates were cleared by centrifugation at 15,000*g* for 30 min at 4 °C.

### 2.4. Electrophoresis and Western blot

Proteins (30–50 μg) were separated by SDS–PAGE using a 5–20% (w/v) linear gradient gel, electrotransferred to a PVDF membrane, fixed with 0.2% (v/v) glutaraldehyde for 10 min, and transiently stained with 0.1% (w/v) Fast Green FCF using standard procedures. The PVDF membranes were blocked with 5% (w/v) bovine serum albumin or 5% (w/v) fat-free powdered milk according to the instructions of the antibodies' manufacturers, and incubated overnight at 4 °C with the primary antibody (1/2000 dilution) and for 1 h at room temperature with the secondary antibody coupled to horseradish peroxidase (1/5000 dilution). The bands were visualized with the ECL reagents following instructions from the manufacturer.

### 2.5. Artificial wound assays

Artificial wounds were done scratching a monolayer of confluent cells with a pipette tip. The plates were washed twice with fresh medium to remove non-adherent cells before photographs were taken at different times using a Nikon Eclipse TS100 microscope at low magnification to follow the repopulation of the wounds. When required, 15 μM W-7 or 15 μM W-13 were added to the medium replacing it daily during the course of the experiment.

### 2.6. Cell motility assays

Cells expressing EYFP-Grb7 or EYFP-Grb7Δ were seeded 24 h post-transfection on 35 mm diameter glass-bottom plates coated with collagen or poly-D-lysine, and their migration was visualized with a Leica TCS SP5 confocal microscope using the 514 nm or 488 nm lasers and a 63× oil-immersion objective. Images were acquired every 10 min for 14 h to generate a time-lapse video using the Leica Microsystem computer software. The extent of migration of individual cells was measured frame-by-frame to determine the average migration rate. Alternatively, cell migration assays across a porous membrane were performed using the Transwell® system.

### 2.7. Cell detachment experiments

Cells were seeded 24 h post-transfection and the rate of detachment determined upon trypsin/EDTA treatment or calcium chelation with 1 mM EGTA counting the number of cells in aliquots of the medium at different times using a Neubauer chamber.

### 2.8. Cytoskeleton analysis

Serum-deprived cells were seeded on fibronectin-coated coverslips and fixed at the times indicated in the legend of the figure with 4% (w/v) paraformaldehyde. Cells were thereafter permeabilized with 0.1% (v/v) Triton X-100, blocked with 2% (w/v) bovine serum albumin overnight at 4 °C, and probed with Alexa Fluor® 488 phalloidin (1:40 dilution) for 1 h at room temperature to detect the actin cytoskeleton. The cells were also stained with DAPI to visualize the nuclei. Coverslips were placed faced-down on microscope slides using ProLong® Gold Antifade mounting solution. Images were acquired with a Leica TCS SP5 confocal microscope using the 488 nm and 358 nm lasers to visualize the actin cytoskeleton and the nuclei, respectively, using a 63× oil-immersion objective and focusing the planes at 1 μm intervals. The images were processed using the Leica Microsystems software.

### 2.9. Statistics

The two-way analysis of variance (ANOVA) and the Student's *t* tests were performed using the GraphPad Prism software program. Data were expressed as the mean ± SEM. Differences were considered significant at $p \leqslant 0.05$ as indicated in the legends of the figures.

## 3. Results

### 3.1. Grb7Δ expression impairs cell motility

As a first approach, we transiently transfected HEK293 cells with pcDNA3.1 (empty vector), pcDNA3/FLAG-Grb7 and pcDNA3/FLAG-Grb7Δ and performed artificial wound assays to follow the closing of the wounds along the time. Fig. 1A shows that

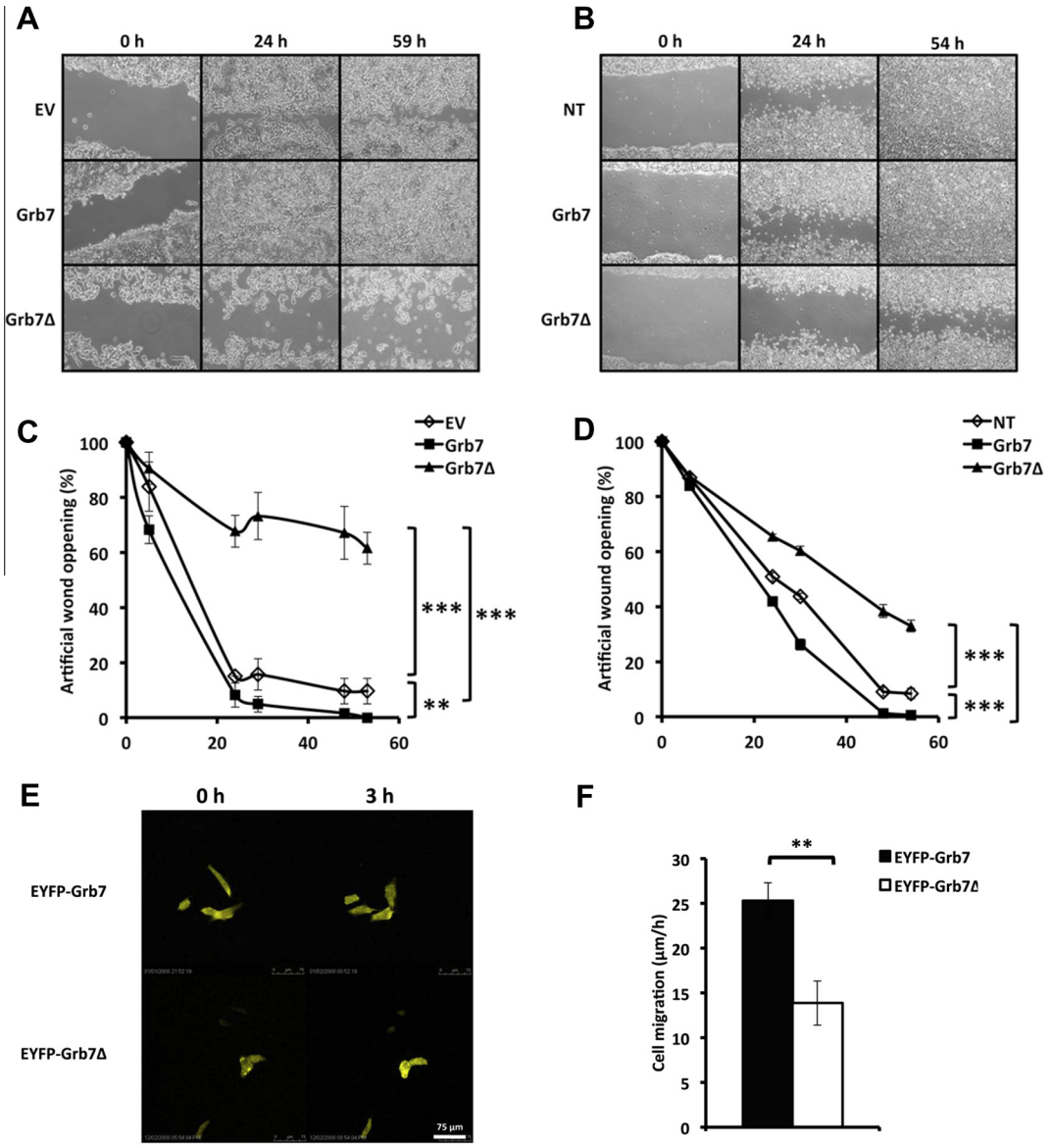


**Fig. 1.** Grb7Δ expression impairs cell migration. (A–D) Artificial wounds were performed in monolayers of confluent HEK293 cells transiently (A and C) and stably (B and D) transfected with the empty vector pcDNA3.1, pcDNA3/FLAG-Grb7 or pcDNA3/FLAG-Grb7Δ. Cells transfected with the empty vector (EV) or non-transfected (NT) cells were used as controls. Photographs were taken at the indicated times to follow the repopulation of the artificial wounds as described in "Materials and Methods". The plots represent the mean ± SEM ($n = 4$) opening of the wound in a set of experiments similar to those shown in the photographs. Significant differences were found when comparing the curves using the two-way ANOVA test ($^{***}p < 0.0001$ and $^{**}p < 0.001$). (E and F) HEK293 cells transiently transfected with pEYFPGrb7 or pEYFP-Grb7Δ were seeded on glass-bottom plates pre-coated with collagen or poly-D-lysine and their motility was observed by time-lapse fluorescence confocal microscopy as described in Materials and Methods. Representative photographs taken three hours apart are shown (E). The plot (F) presents the mean ± SEM rate of migration of individual cells expressing EYFP-Grb7 ($n = 22$) and EYFP-Grb7Δ ($n = 11$). Significant differences were found using the Student's $t$ test ($^{**}p < 0.001$).

transiently transfected cells expressing Grb7 fully closed the wound within 24 h, while the empty vector (EV)-transfected cells closed the wound at a slightly lower rate. However, cells transiently transfected with Grb7Δ failed to close the wound even after 53 h. We performed similar experiments using HEK293 cells stably expressing Grb7 and Grb7Δ. As shown in Fig. 1B, the expression of Grb7Δ also delayed the closing of the artificial wound as compared to non-transfected (NT) or Grb7-expressing cells. In each case the plots show the mean ± SEM wound opening in a set of experiments using transiently (Fig. 1C) and stably (Fig. 1D) transfected cells similar to those shown in the photographs.

To ascertain that the differences found in the wound healing assays were due to differential migration rates and not to different proliferation capacity, we directly measured the motility rate of HEK293 cells transiently transfected with pEYFP-Grb7 or pEYFPGrb7Δ following their movement by time-lapse fluorescence confocal microscopy. Fig. 1E shows typical three hours time-lapsed images of the two transfectants. The plot (Fig. 1F) shows the mean ± SEM motility rate of individual cells in a set of experiments similar to those shown in the photographs. A two-fold lower motility rate of cells expressing EYFP-Grb7Δ as compared to its wild type counterpart is apparent. Similar results were obtained measuring cell migration across Transwell® membranes (*not shown*).

### *3.2. Calmodulin antagonists delay the migration of Grb7-expressing but not of Grb7Δ-expressing or non-expressing cells*

To study the role of CaM on Grb7-mediated cell migration we tested the effect of the cell-permeable CaM antagonists W-7 and

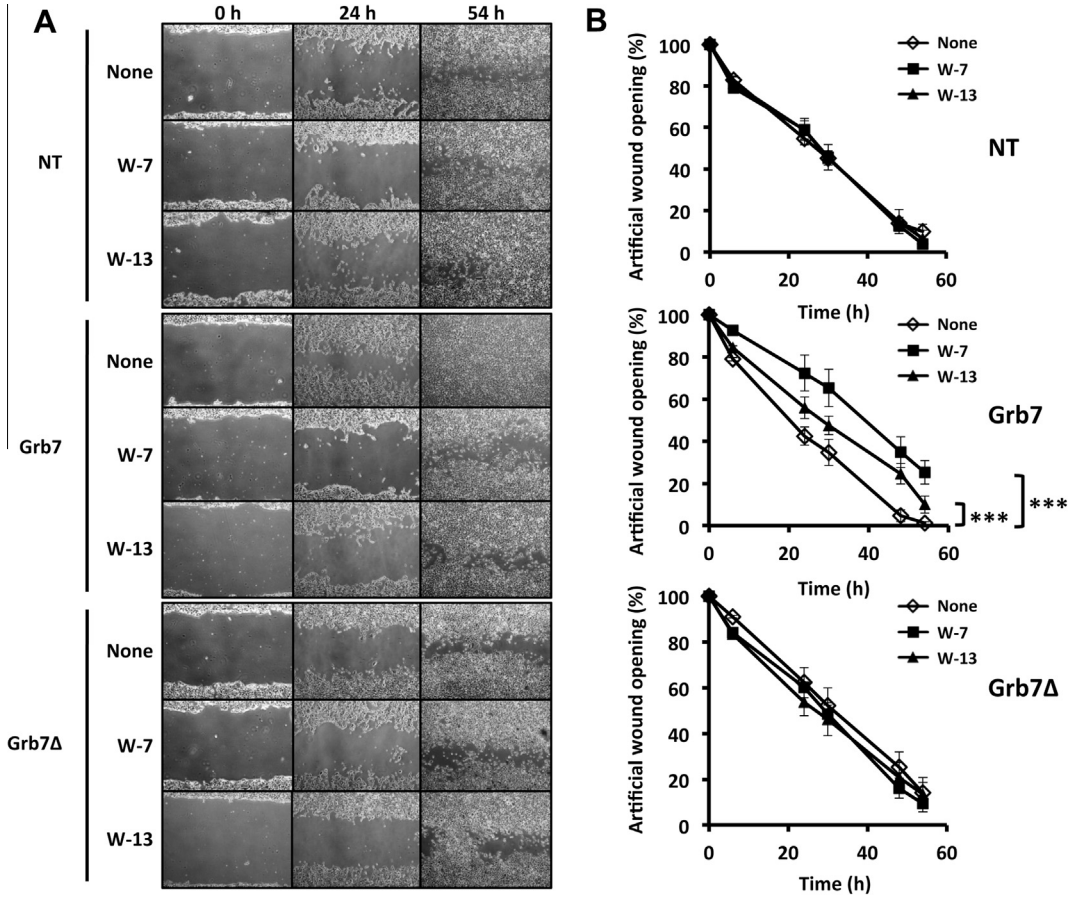


**Fig. 2.** Calmodulin antagonists delay the migration of Grb7-expressing but not of Grb7Δ-expressing or non-expressing cells. Artificial wounds were performed in confluent monolayers of non-transfected (NT) and stably transfected HEK293 cells expressing Grb7 or Grb7Δ treated in the absence (*none*) or in the presence of the CaM antagonists W-7 (15 μM) and W-13 (15 μM). Photographs were taken at the indicated times (A) to follow the repopulation of the wounds as described in Materials and Methods. The plots (B) represent the mean ± SEM ($n = 4$) opening of the wound in the three conditions for each cell type. Significant differences were found when comparing the curves using the two-way ANOVA test ($^{***}p < 0.0001$).

W-13 on non-transfected (NT) and stably transfected HEK293 cells expressing Grb7 and Grb7Δ. Fig. 2A shows that in the presence W-13, and more prominently in the presence of W-7, there was a significant delay in the closing of the wound in Grb7-expressing cells (*middle panels*). In contrast, this effect was absent in Grb7Δ-expressing (*bottom panels*) and non-expressing (*top panels*) cells, suggesting that CaM was involved in Grb7-mediated cell migration. The plots (Fig. 2B) show the mean ± SEM wound opening at progressive times in a set of experiments similar to those shown in the photographs.

### 3.3. Grb7Δ expression impairs cell attachment and cytoskeletal reorganization

A successful migratory event not only requires efficient mechanisms to transiently release the cell from the substrate, but also a proper cytoskeletal reorganization to establish new attachment points at the frontal migratory edge. To study if the observed differences in cell migration described in the previous sections were correlated with deficiency in the attachment/detachment of the cells, we first measured the number of HEK293 cells transiently transfected with pcDNA3.1, pcDNA3/FLAG-Grb7 and pcDNA3/FLAG-Grb7Δ detached upon trypsin plus EDTA treatment (Fig. 3A), routinely used to detach cells for reseeding, or just by chelating extracellular $Ca^{2+}$ with EGTA (Fig. 3B). We observed that both treatments detached cells expressing Grb7Δ more efficiently than cells expressing its wild type counterpart and even more efficiently than control cells transfected with the empty vector (EV).

We directly visualized the reorganization of the actin cytoskeleton by confocal microscopy using phalloidin [16] after seeding cells on fibronectin-coated plates. Fig. 4A shows that non-transfected (NT) and stably transfected HEK293 cells expressing Grb7 developed cytosolic fibrillar structures corresponding to the actin cytoskeleton 15 min after cell seeding and that the cells were completely spread and attached to the fibronectin substrate after 60 min. However, the cells expressing Grb7Δ were unable to develop these fibrillar structures presenting a more circular shape and a peri-cellular organization of the actin cytoskeleton even 60 min after cell seeding and presenting delayed attachment. The cells expressing Grb7Δ, however, were eventually spread and attached to the matrix after longer periods of time (*not shown*).

As the phosphorylation of ERK1/2 has been reported to be involved in the reorganization of the cytoskeleton [17–19], we tested its phosphorylation status. We seeded non-transfected (NT) and stably transfected HEK293 cells expressing Grb7 and Grb7Δ on fibronectin-coated plates and tested the phosphorylation of ERK1/2 and FAK (an upstream signaling component) at different times after cell seeding. Fig. 4B–D shows that FAK was slightly, and ERK1/2 more prominently, phosphorylated (activated) upon seeding. However, the phosphorylation of FAK was somewhat variable but not significantly different among the three cell lines, while the phosphorylation of ERK1/2 was lower and significantly delayed in cells expressing Grb7Δ, as compared to cells expressing

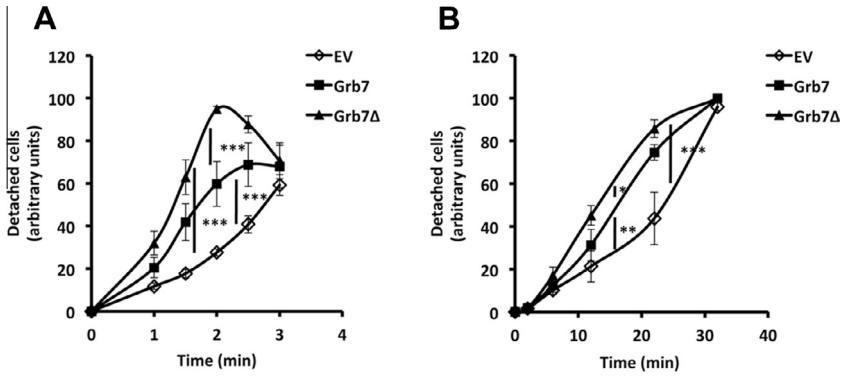


**Fig. 3.** Grb7Δ expression impairs cell attachment. A monolayer of HEK293 cells transiently transfected with the empty vector (EV) pcDNA3.1, pcDNA3/Flag-Grb7 or pcDNA3/Flag-Grb7Δ were detached from the plate either using trypsin/EDTA (A) or 1 mM EGTA (B) and counted as described in Materials and Methods. The plots represent the mean ± SEM ($n = 3$) relative number of detached cells at the indicated times. Significant differences were found when comparing the curves by the two-way ANOVA test (***$p < 0.001$, **$p < 0.01$ and *$p < 0.05$).

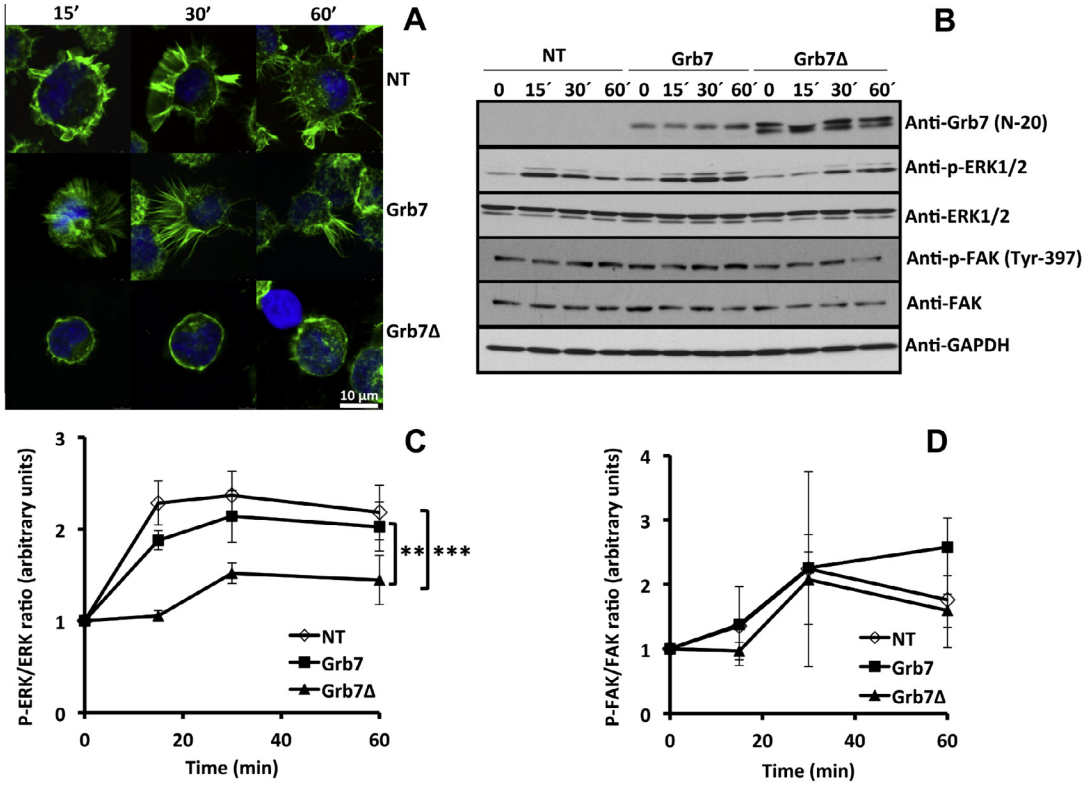


**Fig. 4.** Grb7Δ expression impairs cytoskeletal reorganization. Non-transfected (NT) and stably transfected HEK293 cells expressing Grb7 or Grb7Δ were seeded on fibronectin-coated plates as described in Materials and Methods. (A) The actin cytoskeleton labeled with Alexa Fluor® 488 phalloidin (*green*) and the nuclei stained with DAPI (*blue*) were observed by confocal microscopy as described in Materials and Methods. (B) Cell extracts were collected at the indicated times after seeding and the phosphorylation of ERK1/2 and FAK was analyzed by Western blot using specific antibodies. The GAPDH, ERK1/2 (total) and FAK (total) signals were used as loading controls. The mean ± SEM phospho-ERK/$ERK_{total}$ (C) and phospho-FAK/$FAK_{total}$ (D) ratios were quantified from the densitometric intensities of the bands in three independent experiments as the one shown in B. Significant (***$p < 0.001$ and **$p < 0.01$) (C) and not significant (D) differences among the three cell lines were found when comparing the curves by the two-way ANOVA test.

wild type Grb7 or non-expressing cells. This suggests that Grb7Δ could be blocking the ERK1/2-mediated signaling pathway(s) controlling cytoskeletal reorganization.

## 4. Discussion

Previous studies have shown that upon integrin-mediated stimulation FAK is recruited to focal adhesions triggering its activation and auto-phosphorylation creating docking sites for a variety of intracellular signaling proteins, such as Grb7, paxillin, Src and ERK1/2, resulting in the reorganization of cytoskeleton fibers, triggering a series of not well-defined signaling cascades that end in the promotion of cell migration [9,11,12,17–23]. Grb7 also intervenes in promoting cell migration via the EphB1-ephrin B pathway [10].

In this work, we aimed to study the effect that CaM could exert on the control of Grb7-mediated cell migration. Our data demonstrated that deletion of the CaM-BD of Grb7 impaired cell migration, as HEK293 cells expressing Grb7Δ presented lower migratory rate. This observation was also corroborated in rat gli-

oma C6 cells [15]. The observed difference between cells expressing Grb7 and Grb7Δ was higher when the experiments were performed using transient transfectants as compared to the stable ones. This suggests that the initial overexpression of Grb7 and Grb7Δ occurring in the transient, but not in the stable, transfectants led to a stronger effect.

Although Grb7 is not endogenously expressed in HEK293 cells, we postulate that the deletion of the CaM-BD in the recombinant protein expressed in the cells alters its role as a functional adaptor on their target proteins. The PH domain of Grb7 appears to be important for cell migration, as it facilitates the presence of this adaptor protein in close proximity to the membrane [24]. Moreover, a single mutation in Arg239 impairs Grb7-mediated cell migration by preventing Grb7 binding to phosphoinositides [24]. Although the CaM-BD of Grb7 is located in the proximal region of the PH domain [13], the critical Arg293 is outside the former, suggesting that other regions of the PH domain are also important for Grb7-mediated cell migration. Our laboratory previously described that Grb7Δ lost in great extent the ability to bind to different phosphoinositides, but partially retains the capacity to bind to phosphatidyl-3-phosphate and phosphatidyl-3,5-bisphosphate [13]. This could explain, at least in part, the observed decrease in the migration rate of cells expressing the deletion mutant.

We have also found that CaM appears to be important for Grb7-mediated cell migration, since the cell-permeable CaM antagonists W-13 and W-7 both retarded the migration of Grb7-expressing cells, but not of Grb7Δ-expressing or non-expressing control cells. The stronger inhibitory effect of W-7 with respect to W-13 could be explained by the relatively higher affinity of the former for CaM, as determined measuring their inhibitory capacity on different CaM-dependent systems [13,25,26].

Cell migration is critically dependent on the proper balance between cell attachment and detachment to the extracellular matrix [27]. We demonstrated that HEK293 cells expressing Grb7 presented higher detachment ability than non-expressing control cells. However, cells expressing the deletion mutant Grb7Δ were more easily detached from its substrate as compared to cells expressing its wild type counterpart.

A successful migratory event not only requires efficient mechanisms to release focal adhesions at the rear end of the cell, but also reorganization of the cytoskeleton to generate new attachment points at the frontal migratory edge [27]. After integrin activation by fibronectin it has been described how FAK is activated triggering phosphorylation of ERK1/2 (among other proteins) resulting in the reorganization of the cytoskeletal fibers [17–22,28]. In contrast to earlier data where we could not detect differences in the structure of the cytoskeleton of static cells expressing Grb7 versus Grb7Δ [13], our present results showed that Grb7Δ-expressing cells present altered cytoskeletal reorganization associated to the dynamic process of cell attachment to fibronectin, as compared to cells expressing wild type Grb7, and this is associated to lower and delayed phosphorylation of ERK1/2. However, we obtained no significant differences in the phosphorylation levels of FAK between Grb7Δ and Grb7expressing cells. The fact that FAK is phosphorylated upstream of Grb7 suggests that Grb7Δ could be correctly recruited to the signaling complex but somehow the proper transmission of the signal downstream the ERK1/2 pathway was delayed and partially blocked.

The cell migration rate is enhanced when the strength of cell adhesion molecules for the extracellular matrix is neither too strong nor too weak [29]. In this context, we hypothesized that Grb7Δ-expressing cells present a higher tendency to detached from its substrate because they may have more labile and/or a lower number of anchoring points. This, in conjunction with deficiencies in cytoskeletal reorganization during cell attachment to the extracellular matrix, offers not enough mechanical support for cell motility resulting in aborted or defective migration.

## Acknowledgments

This work was funded in part by Grants (to AV) from the *Secretaría de Estado de Investigación Desarrollo e Innovación* (SAF2011-23494), the *Consejería de Educación de la Comunidad de Madrid* (S2010/BMD-2349), and the European Commission (contract PITN-GA-2011-289033). IG-P was supported by a fellowship from the *Ministerio de Educación Cultura y Deporte*.

## References

[1] B. Margolis, The GRB family of SH2 domain proteins, Prog. Biophys. Mol. Biol. 62 (1994) 223–244.
[2] R.J. Daly, The Grb7 family of signaling proteins, Cell. Signal. 10 (1998) 613–618.
[3] D.C. Han, T.L. Shen, J.L. Guan, The Grb7 family proteins: structure, interaction with other signaling molecules and potential cellular functions, Oncogene 20 (2001) 6315–6321.
[4] A. Villalobo, H. Li, J. Sánchez-Torres, The Grb7 protein family, Curr. Top. Biochem. Res. 5 (2003) 105–114.
[5] T.L. Shen, J.L. Guan, Grb7 in intracellular signaling and its role in cell regulation, Front. Biosci. 9 (2004) 192–200.
[6] E. Lucas-Fernández, I. García-Palmero, A. Villalobo, Genomic organization and control of the Grb7 gene family, Curr. Genomics 9 (2008) 60–68.
[7] J. Manser, W.B. Wood, Mutations affecting embryonic cell migrations in *Caenorhabditis elegans*, Dev. Genet. 11 (1990) 49–64.
[8] J. Manser, C. Roonprapunt, B. Margolis, *C. elegans* cell migration gene mig-10 shares similarities with a family of SH2 domain proteins and acts cell nonautonomously in excretory canal development, Dev. Biol. 184 (1997) 150–164.
[9] D.C. Han, J.L. Guan, Association of focal adhesion kinase with Grb7 and its role in cell migration, J. Biol. Chem. 274 (1999) 24425–24430.
[10] D.C. Han, T.L. Shen, H. Miao, B. Wang, J.L. Guan, EphB1 associates with Grb7 and regulates cell migration, J. Biol. Chem. 277 (2002) 45655–45661.
[11] D.C. Han, T.L. Shen, J.L. Guan, Role of Grb7 targeting to focal contacts and its phosphorylation by focal adhesion kinase in regulation of cell migration, J. Biol. Chem. 275 (2000) 28911–28917.
[12] T.L. Shen, J.L. Guan, Differential regulation of cell migration and cell cycle progression by FAK complexes with Src, PI3K, Grb7 and Grb2 in focal contacts, FEBS Lett. 499 (2001) 176–181.
[13] H. Li, J. Sánchez-Torres, A.F. del Carpio, A. Nogales-González, P. Molina-Ortiz, M.J. Moreno, K. Török, A. Villalobo, The adaptor Grb7 is a novel calmodulin-binding protein: functional implications of the interaction of calmodulin with Grb7, Oncogene 24 (2005) 4206–4219.
[14] I. García-Palmero, A. Villalobo, Calmodulin regulates the translocation of Grb7 into the nucleus, FEBS Lett. 586 (2012) 1533–1539.
[15] I. García-Palmero, P. López-Larrubia, S. Cerdán, A. Villalobo, Nuclear magnetic resonance imaging of tumor growth and neovasculature performance *in vivo* reveals Grb7 as a novel antiangiogenic target, NMR Biomed. (2003), http://dx.doi.org/10.1002/nbm.2918.
[16] E. Wulf, A. Deboben, F.A. Bautz, H. Faulstich, T. Wieland, Fluorescent phallotoxin, a tool for the visualization of cellular actin, Proc. Natl. Acad. Sci. USA 76 (1979) 4498–4502.
[17] R.L. Klemke, S. Cai, A.L. Giannini, P.J. Gallagher, P. de Lanerolle, D.A. Cheresh, Regulation of cell motility by mitogen-activated protein kinase, J. Cell Biol. 137 (1997) 481–492.
[18] D.D. Schlaepfer, S.K. Mitra, D. Ilic, Control of motile and invasive cell phenotypes by focal adhesion kinase, Biochim. Biophys. Acta 1692 (2004) 77–102.
[19] S.K. Mitra, D.A. Hanson, D.D. Schlaepfer, Focal adhesion kinase: in command and control of cell motility, Nat. Rev. Mol. Cell Biol. 6 (2005) 56–68.
[20] M.D. Schaller, C.A. Borgman, B.S. Cobb, R.R. Vines, A.B. Reynolds, J.T. Parsons, pp125$^{FAK}$, a structurally distinctive protein-tyrosine kinase associated with focal adhesions, Proc. Natl. Acad. Sci. USA 89 (1992) 5192–5197.
[21] E.A. Clark, J.S. Brugge, Integrins and signal transduction pathways: the road taken, Science 268 (1995) 233–239.
[22] B.D. Cox, M. Natarajan, M.R. Stettner, C.L. Gladson, New concepts regarding focal adhesion kinase promotion of cell migration and proliferation, J. Cell. Biochem. 99 (2006) 35–52.
[23] P.Y. Chu, L.Y. Huang, C.H. Hsu, C.C. Liang, J.L. Guan, T.H. Hung, T.L. Shen, Tyrosine phosphorylation of growth factor receptor-bound protein-7 by focal adhesion kinase in the regulation of cell migration, proliferation, and tumorigenesis, J. Biol. Chem. 284 (2009) 20215–20226.
[24] T.L. Shen, D.C. Han, J.L. Guan, Association of Grb7 with phosphoinositides and its role in the regulation of cell migration, J. Biol. Chem. 277 (2002) 29069–29077.
[25] H. Hidaka, T. Tanaka, Naphthalenesulfonamides as calmodulin antagonists, Methods Enzymol. 102 (1983) 185–194.

[26] W.C. Hope, T. Chen, D.W. Morgan, Secretory phospholipase A2 inhibitors and calmodulin antagonists as inhibitors of cytosolic phospholipase A2, Agents Actions 39 (1993) C39–C42.
[27] D.A. Lauffenburger, A.F. Horwitz, Cell migration: a physically integrated molecular process, Cell 84 (1996) 359–369.
[28] R.O. Hynes, Integrins: bidirectional, allosteric signaling machines, Cell 110 (2002) 673–687.
[29] S.L. Gupton, C.M. Waterman-Storer, Spatiotemporal feedback between actomyosin and focal-adhesion systems optimizes rapid cell migration, Cell 125 (2006) 1361–1374.